Fracture Properties of Epoxy/Poly(styrene-*co*-allylalcohol) Blends

A. Salazar, S. G. Prolongo, J. Rodríguez

Departmento. de Ciencia e Ingeniería de Materiales, Escuela Superior de Ciencias Experimentales y Tecnología, Universidad Rey Juan Carlos, C/Tulipán, s/n. 28933 Móstoles, Madrid, Spain

Received 20 November 2006; accepted 23 February 2007
DOI 10.1002/app.26811
Published online 15 August 2007 in Wiley InterScience (www.interscience.wiley.com).

ABSTRACT: The epoxy/polystyrene system is characterized by a poor adhesion between the constituent phases, which determines its mechanical properties. The adhesion can be improved via blends based on epoxy resin and random copolymers, poly(styrene-*co*-allylalcohol) (PS-*co*-PA). In this work, the influence of PS-*co*-PA content and the good adhesion between the phases on the tensile properties and the fracture toughness achieved through instrumented Charpy tests have been investigated. The tensile strength and the deformation at break showed an increase in the PS-*co*-PA content while the Young's modulus remained the same. The tensile fracture surfaces revealed that the improvement of these magnitudes was mainly due to a crack deflection mechanism. Also, the fracture toughness of the blends was superior to that of the pure epoxy resin. The main operating toughening mechanism was crack deflection. The fractographic analysis showed that $\sim$ 80% of the particles were broken, and the crack tended to divert from its original path through the broken PS-*co*-PA particles. The remaining particles were detached from the epoxy resin, and the holes left suffered plastic deformation. Analytical models were used to predict successfully the toughness due to these mechanisms. © 2007 Wiley Periodicals, Inc. J Appl Polym Sci 106: 3227–3236, 2007

Key words: epoxy resin; copolymer/epoxy blends; tensile properties; fracture toughness; micromechanisms of failure

INTRODUCTION

Epoxy resins are highly demanded for engineering applications in the field of structural adhesives, matrix for fiber composite materials, and coatings due to their high thermal, chemical, and mechanical resistance, and good electrical properties. However, their main drawback is their inherent brittleness, which implies poor fracture toughness, poor resistance to crack propagation, and low impact strength. These attributes have hindered their use in structural applications.[1] Rubber toughening of epoxies is one common method to improve the fracture toughness, which has met some success.[2–7] However, the improvements in fracture toughness of these rubber-modified epoxies are accompanied by a significant drop in stiffness and strength, and often lower T_g, when compared with the pure epoxy resin.[2,4,6,8]

The way to improve their mechanical and fracture behavior without major loss in other desirable properties is to insert high performance engineering thermoplastics into the high cross-link epoxy network.[8] Polystyrene is a thermoplastic with high mechanical and chemical resistance,[9] but it is usually not used as an epoxy hardener modifier due to its high thermodynamic incompatibility, which generates large thermoplastic domains with poor matrix adhesion.[10] Even though, recent works by Korenberg et al.[11] and Johnsen et al.[12] have reported the improvements in the fracture toughness of an epoxy polymer blended with a semicrystalline polystyrene, which shows a poor adhesion between the constituent phases. Complete phase separation was undergone via two thermal-processing histories. Three different microstructures were obtained depending on the thermal-processing history and the polystyrene content. The highest fracture toughness values were related to the polystyrene particle phase separation (1–4 μm in diameter) microstructure, and the toughening micromechanism was due to polystyrene debonding, poor adhesion between the thermoplastic phase and the epoxy matrix, followed by plastic void growth of the surrounded epoxy matrix.

Although there are many factors, which influence the toughening process of thermoplastic blended epoxies, the resin-thermoplastic interface seems to play an important role in the toughening mechanisms. With the exception of the results presented by Korenberg et al.[11] and Johnsen et al.,[12] the majority of the works in the literature state that a strong interface, which can withstand the loads placed upon it, guarantees a drawing mechanism of the thermoplastic particles and consequently, an improvement in the fracture toughness of the system.

Correspondence to: A. Salazar (alicia.salazar@urjc.es).

Journal of Applied Polymer Science, Vol. 106, 3227–3236 (2007)

Bucknall and Gilbert[13] studied a DDS-cured, tetrafunctional epoxy modified by PEI, and the fracture toughness of this system increased significantly with the PEI content. The microstructure was formed by thermoplastic particles (2 μm in diameter) at low PEI content, which became large domains at higher PEI addition. The toughening effect was related to ductile drawing of the thermoplastic phase due to the strong epoxy-plastic interface. Frounchi[14] observed this very same toughening mechanism operating in PADC/PEMA blends and so Hedrick et al.[15] and Hourston and Lane[16] in a DDS-cured DGEBA modified by PES and in a DDS-cured TGPAP modified by PEI, respectively. Cardwell and Yee[17] pointed out that the important factors, which influence toughening by thermoplastic modifiers may be hindered by the method the samples were prepared, phase inversion, and cocontinuous networks with increasing amounts of thermoplastic modifier. To eliminate these problems, they designed a system using preperformed polyamide-12 particles to keep the morphology constant over various concentrations of this second phase. The matrix employed were DDM-cured and piperidine-cured DGEBA resins. The fracture toughness increased with the thermoplastic content in both epoxy matrix, and this improvement was due to a crack bridging mechanism, involving a large plastic deformation of the second phase.

To increase the adhesion between the thermoplastic domains and the epoxy resin, some studies have been reported on blends with thermoset precursor and thermoplastic copolymer modifier.[18,19] In this work, a poly(styrene-*co*-allylalcohol) (PS-*co*-PA) random copolymer is used as an epoxy modifier with the aim of investigating the influence of a good adhesion between the polystyrene and the epoxy matrix in the mechanical and fracture properties. Prolongo et al.[20] reported the presence of an interfacial layer, 150-nm thick, in these very blends and concluded that this layer should contribute to improve the adhesion between the phases. The interphase was originated by hydroxyl/epoxy interaction and its thickness seemed to be independent of the modifier content.

This work is concerned with the investigation of the mechanical properties and fracture toughness of thermoset epoxy resin with a PS-*co*-PA copolymer as a modifier. The mechanical response of this system was evaluated through tensile tests. Fracture toughness performances were achieved in single-edge notched bend (SENB) specimens through instrumented Charpy impact tests.

EXPERIMENTAL

Materials

The studied blend was composed of an epoxy resin modified with different amounts of random copolymers of polystyrene with 40% of polyallylalcohol (PS-*co*-PA). The epoxy precursor used was diglycidyl ether of bisphenol A (DGEBA), supplied by Ciba under the commercial name of Araldite F. Its epoxy equivalent weight is 178 g/eqiv, which was measured by the chemical titration of the end groups. As a curing agent, we used 4,4′-diaminodiphenyl sulfone (DDS), acquired from Sigma–Aldrich Chemical. A linear PS-*co*-PA copolymer supplied by Sigma–Aldrich was used as modifier. It was characterized by a low molar mass and 40 wt % allyl content. Its number–average molecular weight was 1200 g/mol, and presented a polydispersity index close to 1.8.

The manufacture process consisted of the following steps. First, homogeneous solutions of different amount of PS-*co*-PA (from 5 to 20 wt %) in epoxy monomer were prepared using a magnetic stirrer at 140°C in vacuum for 30 min. The curing agent was then added to the mixture in a stoichiometric epoxide/amine ratio, and mechanical mixing was continued for a few more minutes, at 180°C in vacuum. The mixing continued until the amine hardener was totally dissolved. Immediately after, it was poured into a steel mold, which was previously treated with an antiadherent demold agent, MARBOCOTE 445 ECO. Afterward, the mold was inserted into heating plates for curing. The curing treatment consisted of a heating at 210°C during 3 h. The specimens were cooled down at room temperature inside the heating plates to avoid the crack formation due to thermal shock.

Mechanical properties

Tensile tests

The tensile tests were carried out, following the ASTM D638 standard, to measure the tensile strength, the Young's modulus, and the deformation at break in the epoxy resin, and the blends with different thermoplastic contents. Type I specimens with $13 \times 57 \times 3$ mm^3 in the narrow section were tested on an electromechanical testing machine (MTS Alliance RF/100), under displacement control at a crosshead speed of 1 mm/min. The strain was measured during the tests with an extensometer attached to the sample (model MTS 654-12F).

Fracture properties

Fracture toughness at impact tests was carried out on SENB specimens obtained directly from the mold with $6 \times 18 \times 79$ mm^3 in size and an initial notch length of 8.1 mm. A natural crack could not be inserted by tapping at the center of the notch due to the brittleness of the materials. Thus, a sharp crack was generated at the center of the notch with a cop-

per disk 0.05-mm thick mounted on a microcutting machine Struers Accutom-5. The resulting notch was ~ 9.0 mm in depth.

The fracture toughness tests were carried out on an instrumented Charpy impact pendulum (Ceast Resil Impactor), following the guidelines described by ESIS TC4 Protocol for the determination of fracture toughness at moderately high loading rates.[21] All the materials were tested at a load-point displacement rate of 0.3 m/s, and this condition was accomplished with a 4 J striker positioned at drop height of 4.6 mm. The associated impact energy was of 42.9 mJ. The support span was of 72 mm for all the materials.

After the mechanical tests, the fracture surfaces of the broken specimens were examined by environmental scanning electron microscope, ESEM (Philips XL30), to determine the micromechanisms of failure. The fractographic images obtained were also used to evaluate the percentage of broken, intact, and detached particles as well as to measure the diameter of the particles and the deformation of the matrix. These quantitative measurements were performed with Image Pro-Plus 4.5 image analysis software.

The interphase between the constituent phases of this system was analyzed via transmission electron microscope, TEM (Phillips Tecnai 20). The specimens were cut at room temperature using an ultramicrotome (Leica EMFCS) equipped with a diamond knife. The resulting ultrathin sections were picked up on copper grids and stained in the vapor of an aqueous solution of RuO_4.

RESULTS AND DISCUSSION

Morphology

The micrographs associated to the epoxy resin and the systems formed by the blends with 10 and 20 wt % PS-*co*-PA are shown in Figure 1(a–c), respectively. The microstructure consisted of PS-*co*-PA spherical domains homogenously dispersed into the epoxy matrix. The size of the domains scarcely increased with the PS-*co*-PA content and the average diameter of the separated phase was close to 2 μm.[20]

The thermomechanical response of this system has been extensively studied in the work reported by Prolongo et al. [20,22] The DMTA experiments carried out in these blends revealed the presence of two α relaxations, which confirms the heterogeneity of these blends. Besides, while the T_α associated to the relaxation of the PS-*co*-PA (~ 80°C) maintained constant independently of the content in the blend. The high T_α associated with the cured epoxy resin decreased from 243.4°C for the pure epoxy resin to 217.8°C in the case of the blend with 20 wt % of PS-*co*-PA. This diminish was due to the partial miscibility of the PS-*co*-PA on the epoxy network.[20]

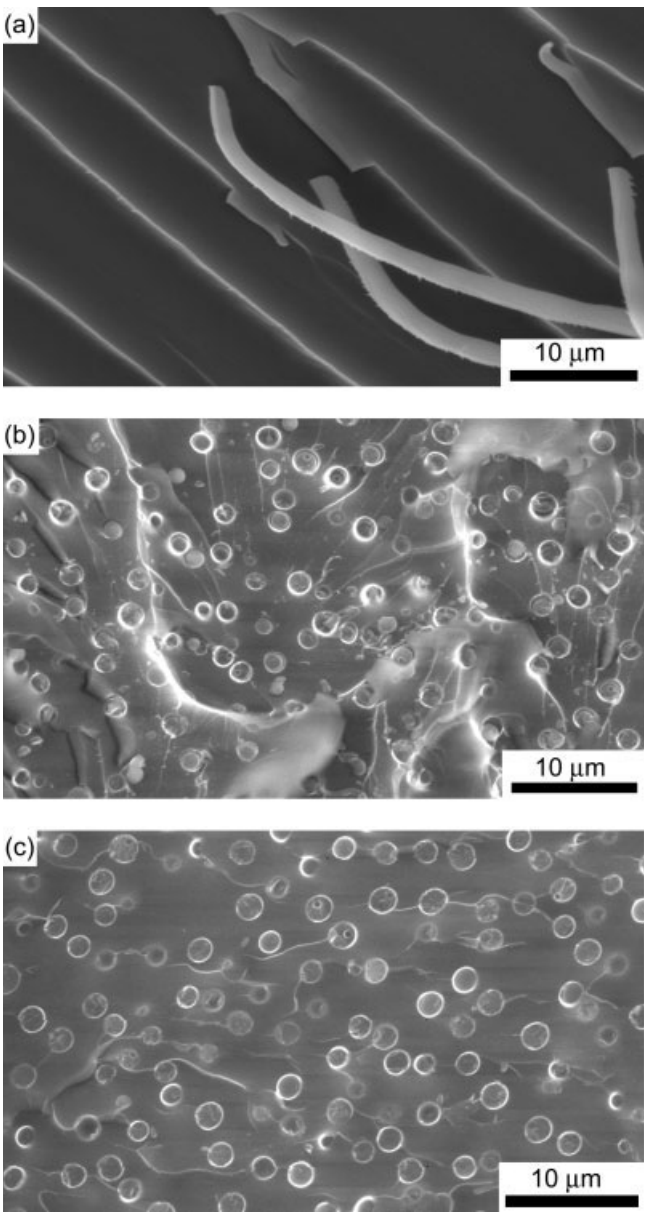

Figure 1 Micrographs showing the morphology of the epoxy resin (a), blends with 10 wt % of PS-*co*-PA (b), and with 20 wt % of PS-*co*-PA (c).

The chemical structure of the blends and the appearance of the epoxy-hydroxyl reaction have been studied in the work by Prolongo et al.[22] through FTIR and ^{13}C NMR experiments.

Mechanical properties

Tensile properties

The Young's modulus, E, the tensile strength, σ, and the deformation at break, ε, are plotted as a function

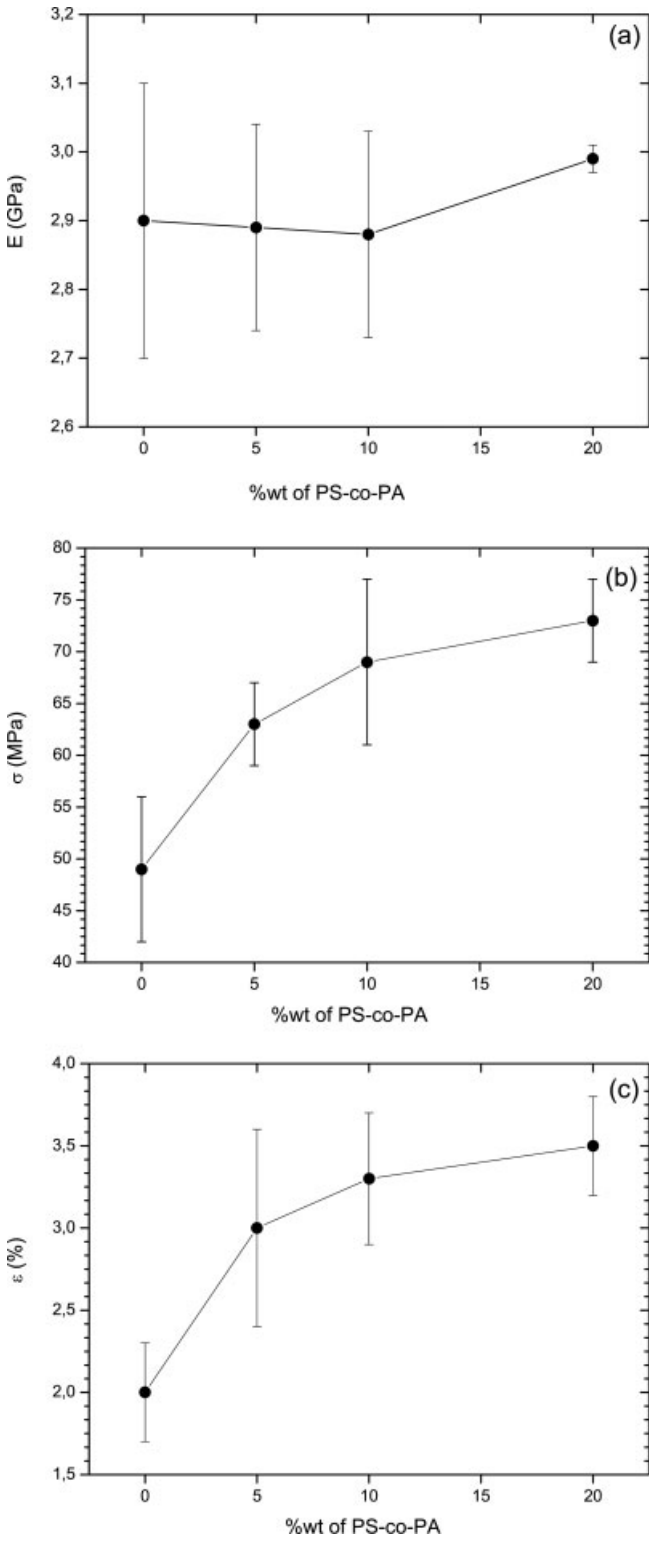

Figure 2 Evolution at room temperature of the Young's modulus (a), the tensile strength (b), and the deformation at break (c) with the PS-*co*-PA content.

of the PS-*co*-PA content in Figure 2(a–c), respectively. The plots include the average values and the standard deviations corresponding to six tests for the epoxy resin and the blends with different thermoplastic contents. All the load-deformation curves, independently of the thermoplastic content, were basically linear and elastic till fracture. Some conclusions can be drawn from the results. First, over the investigated composition range, the addition of PS-*co*-PA did not change the Young's modulus of the resin [Fig. 2(a)]. The scatter obtained in the measurements of the Young's modulus of the epoxy resin and the blends with a 5 and 10% of thermoplastic content was so high that the moderate increase observed in the average value of the blend with 20% is not reliable. The value of the Young's modulus of the epoxy resin is in agreement with the flexural values reported by previous researchers,[15,23–25] and the tensile module reported by Grillet et al.[26] Even so, the tendency of the Young's modulus with the PS-*co*-PA content obtained from the tensile tests differs with that measured via DMTA experiments in this very system by Prolongo et al.[20] There, the storage modulus in the glassy state increased from 2.55 GPa for the pure epoxy resin to 2.75 GPa for the blends with 20 wt % of PS-*co*-PA. The discrepancy in the values obtained by these two methods is due to the inherent difficulty of measuring the Young's modulus. Second, the tensile strength and the deformation at break increased with the PS-*co*-PA content [Fig. 2(b,c)]. The maximum improvement was achieved when the concentration of PS-*co*-PA is of 20 wt %, with values 15% higher than those for the epoxy resin.

The fracture surfaces of the broken specimens for the epoxy resin and the blends with 5 wt % of thermoplastic content obtained from tensile tests are shown in Figures 3 and 4, respectively. All the fracture surfaces tested were flat. The epoxy resin and the blends showed large pores ($\sim$ 200 μm), easily observed at low magnification, and marked with an arrow [Figs. 3(a) and 4(a)], principally concentrated at the corners of the specimens. These large defects with the same dimensions are present in all the specimens, independently of the PS-*co*-PA content. These pores were originated during the sample manufacture when the mixture was poured into the steel mold. Because of the viscosity of the mixture, the corners of the mold were not filled conveniently, and bubbles of air were trapped at the corners of the mold. The fracture surface of the epoxy resin showed accentuated river markings and many ridges, pointing to the defect responsible for the failure [Fig. 3(a)],[27] as well as some features protruding from the fracture surface usually named ''stacked lamellar texture''[28,29] (indicated by a circle) [Fig. 3(c)]. Although the fracture is predominantly brittle, these features imply the fortuitous intersection of two planes of fracture, stating the presence of localized plastic deformation in a highly crosslinked network. This phenomenon was also observed by Atsuta and

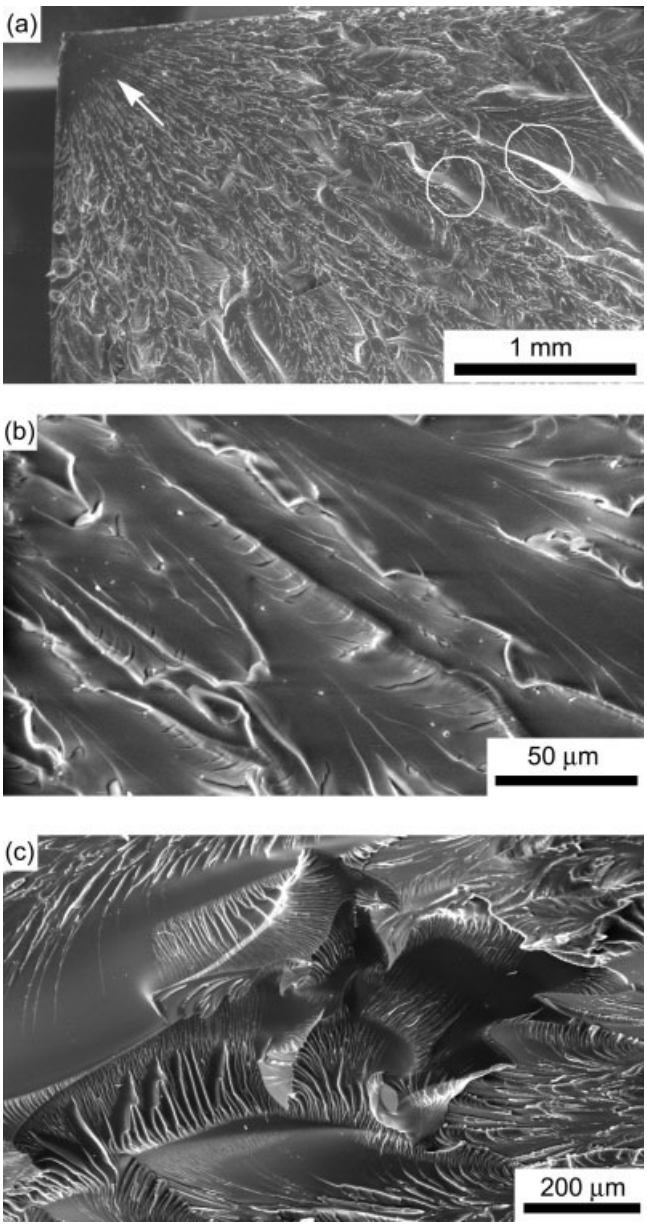

Figure 3 Fracture surface of the epoxy resin broken in tensile tests: (a) low magnification micrograph where pore is marked with an arrow and features protruding from the surfaces are marked with circles, (b) detail of river markings, and (c) detail of the outgoing prominences from the surface with an array of tracks.

Turner,[28] Robertson and Mindroiu,[29] and Fiedler et al.[30]

Little differences were found among the fracture surfaces of the specimens with 5, 10, and 20 wt % PS-*co*-PA content. Although the failure was also brittle and the crack was nucleated by a pore, the fracture surface was much rougher [Fig. 4(b)] compared with that of the epoxy resin [Fig. 3(b)], and the river markings were not so easy to see as the additive content increased. So, these differences indicate that the particles play an important role during the crack propagation. The deviation of the crack front from its original plane showed that the particles may act as obstacles, changing the propagation rate and generating this sheetlike structure that is accompanied by particles breakage and matrix yielding [Fig. 4(c)]. This crack deflection mechanism is responsible for the increase in the tensile strength and deformation at break of the blends as more energy is required to enlarge the area of the crack. Although this mechanism of failure operates mainly with inorganic fillers,

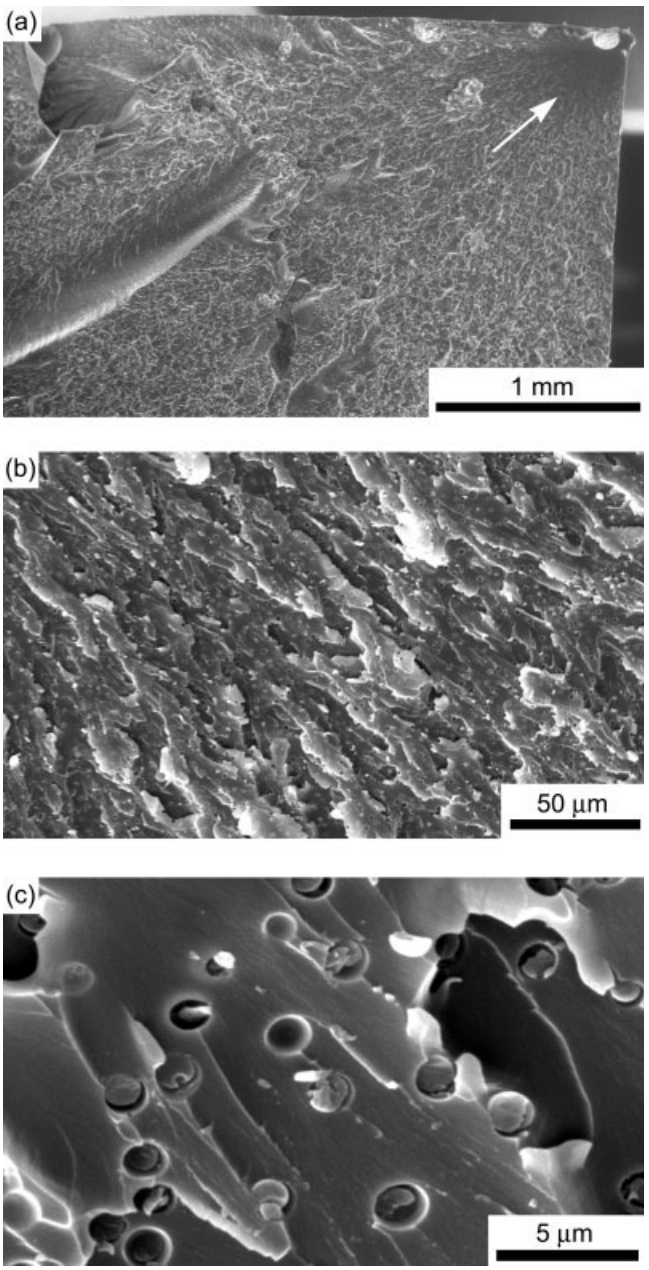

Figure 4 Fracture surface of the blend with 5% of PS-*co*-PA content broken in tensile tests: (a) low magnification micrograph where the pore is marked with an arrow, (b) detail of rough surface, and (c) high magnification micrograph showing particles breakage and matrix yielding.

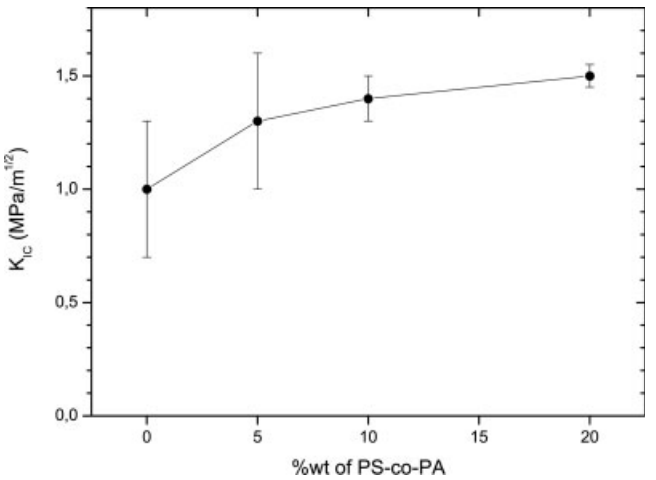

Figure 5 Fracture toughness as a function of the PS-*co*-PA content.

it also has an important contribution when high modulus thermoplastic particles are used as modifiers. This has been proved by Abad et al.[27] in tensile fracture surfaces of BAC-cured DGEBA resin with a BAC modifier, by Korenberg et al.[11] and Johnsen et al.[12] in the system formed by MCDEA-cured DGEBA with syndiotactic polystyrene modifier and by Francis et al.[31] in the epoxy/PEEKMOH system.

Fracture properties

The fracture toughness is plotted as a function of the PS-*co*-PA content in Figure 5. The graph includes the average values and the standard deviations corresponding to five tests for the epoxy resin and the blends with different PS-*co*-PA content. The fracture toughness increased with the PS-*co*-PA content. The maximum improvement achieved at 20 wt % was 50% higher than that for the epoxy resin.

The fracture toughness of the epoxy resin is slightly higher than that found in the literature,[8,11,12,23,25,26] and so this leads to have to consider the possible effect of the notch radius. All the fracture specimens presented a notch radius of $\sim$ 40 μm via sawing as a natural crack of proper length was difficult to grow and control via tapping in these brittle materials. In principle, this radius can lead to overestimate the actual fracture toughness of the materials. To study the possible influence of the notch-root radius on the fracture toughness measurements of these blends, the guidelines reported by Damani et al.[32] and Picard et al.[33] for brittle materials were followed. It was checked that a notch radius $\sim$ 40 μm is below the threshold for which the fracture toughness is sensitive to the notch-root radius.

The fracture surfaces of the broken specimens for the epoxy resin and the blends with 10 wt % of PS-*co*-PA content are shown in Figures 6 and 7, respectively. The epoxy resin showed a fairly smooth and featureless surface [Fig. 6(a)]. The only remarkable feature was some fine cracks located next to the notch [Fig. 6(b)]. The blends with 10 and 20 wt % of PS-*co*-PA content were very similar and were characterized by a rough surface [Fig. 7(b)], which extended in a small area around the crack tip [Fig. 7(a)]. The study at higher magnification also revealed the occurrence of crack deflection [Fig. 7(c)] as well as a high amount of broken particles and matrix deformation around these broken particles via plastic void formation [Fig. 7(d)]. All the particles presented a void, which should have been generated during the curing process as air bubbles, coming from the solution, were trapped inside the thermoplastic particles.

The percentage of broken particles and detached or intact particles as a function of the PS-*co*-PA content is plotted in Figure 8. The plot includes the average values and the corresponding standard errors of the broken and detached or intact particles corresponding to the measurements of five micrographs taken at a magnification of 5000 for the blends with 5, 10, and 20 wt % of PS-*co*-PA. The graph indicates that around 80% of the particles are broken. The high number of broken particles points out the presence of a strong interphase between the matrix and

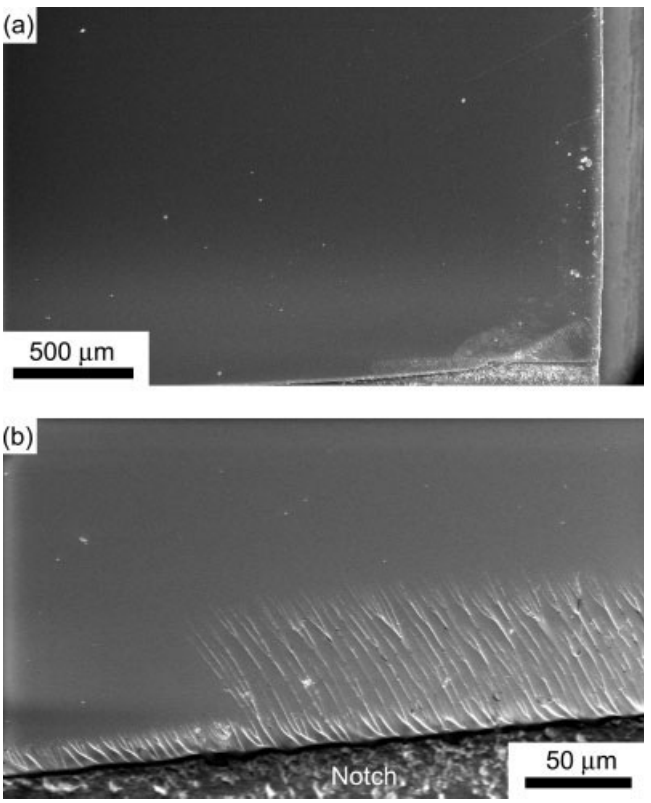

Figure 6 Fracture surface of the epoxy resin broken in dynamic fracture toughness test: (a) panoramic view and (b) detail of some fine cracks next to the notch.

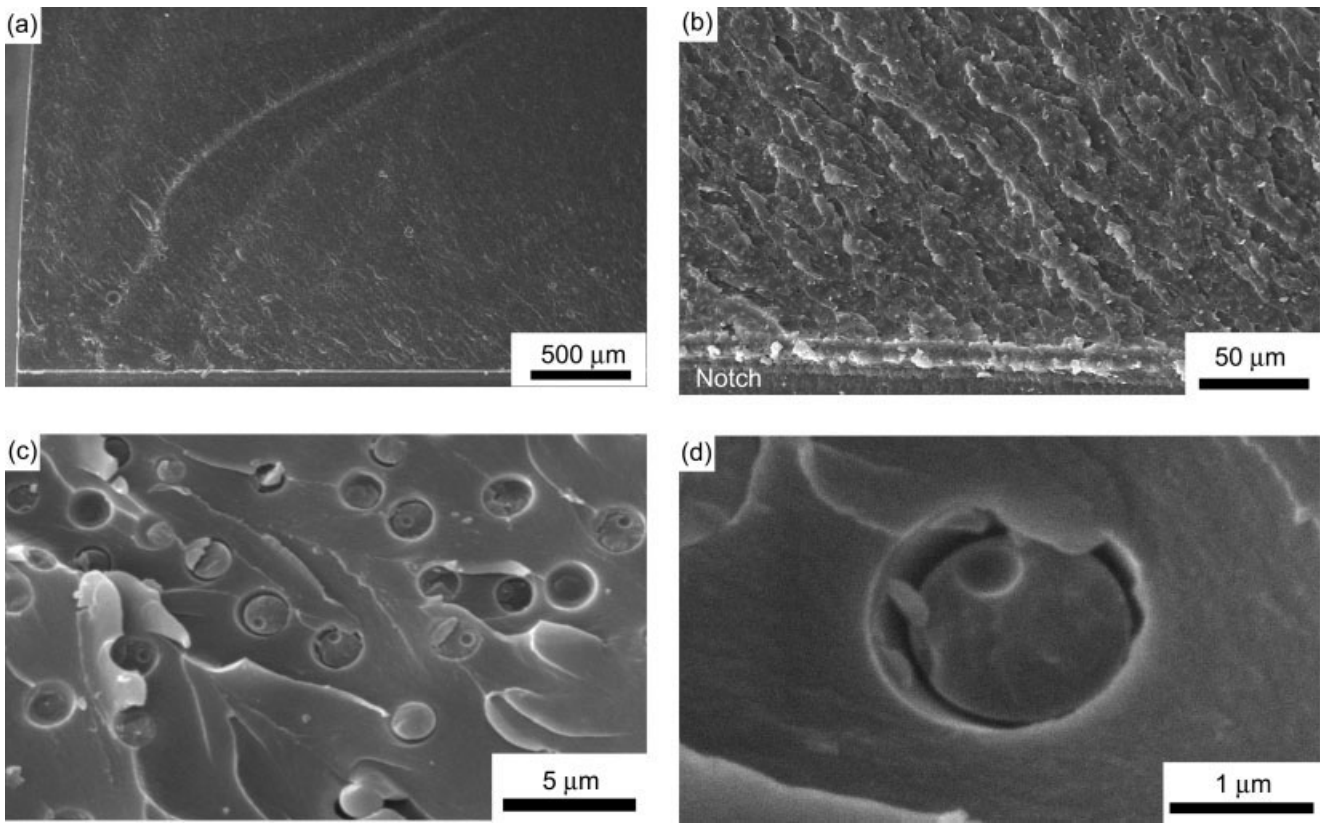

Figure 7 Fracture surface of the blend with 10% of PS-*co*-PA content broken in dynamic fracture toughness tests: (a) panoramic view, (b) micrograph taken around the crack tip, (c) high magnification micrograph in which most of the particles are broken, and (d) detail of a broken particle surrounded by cavities.

the particles. The existence of an interfacial layer $\sim$ 100–150-nm thick between the matrix and the PS-*co*-PA particles in this system is shown via TEM analysis in Figure 9.

To enhance the fracture toughness, not only two phase morphology is desirable but also a good interaction between the dispersed phase and the epoxy resin is essential. This has been accomplished by the incorporation of a copolymer to the polystyrene modifier. The mechanical response exhibited by the blends was improved compared with the epoxy resin and the main mechanism exhibited was crack

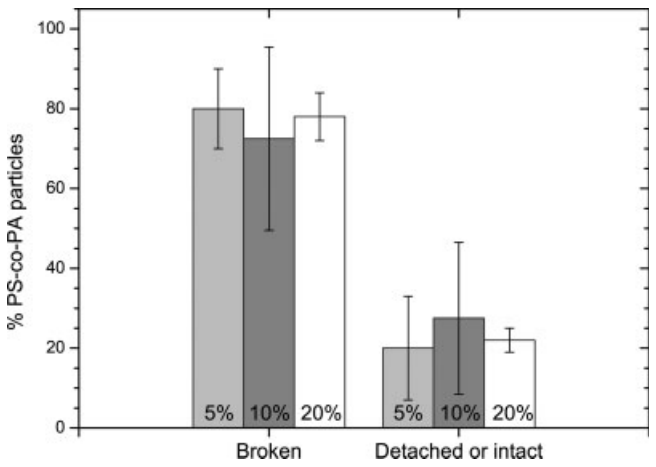

Figure 8 Percentage of broken and detached or intact PS-*co*-PA particles measured from the fracture toughness surfaces of the blends with 5, 10, and 20% PS-*co*-PA content.

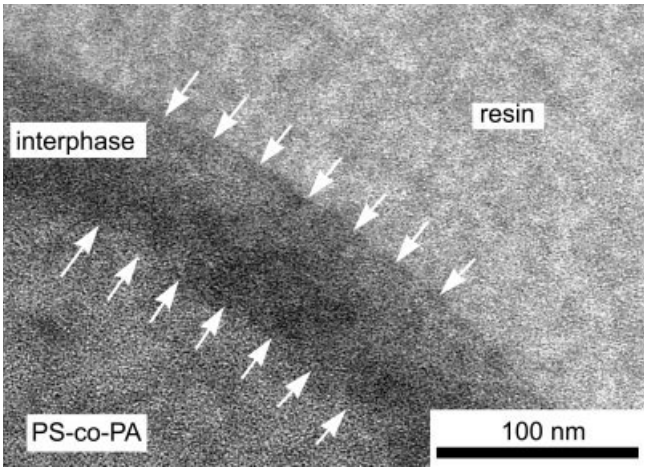

Figure 9 TEM micrograph showing the interphase between the matrix and the PS-*co*-PA particles for the blend with 20 wt % of PS-*co*-PA. The interphase outline is marked with arrows.

deflection closely related to the breakage of particles. In a lesser extent, plastic void formation due to matrix deformation around the particles also contributed to the fracture toughness improvement. This mechanism is principally related to the detached particles as Johnsen et al.[12] demonstrated that the plastic void growth was the main operating contribution when the adhesion between the dispersed particles and the matrix was very poor.

Modeling of the toughening micromechanisms

Huang and Kinloch[34] developed a model to predict the toughening effect of a particulate thermoplastic blend, which involves the main energy-dissipating toughening mechanisms. This model assumes that the fracture behavior is linear-elastic and the plastic zone is small compared to the dimensions of the specimens. The fracture energy in a thermoplastic modified polymer can be expressed as

$$G_{IC} = G_{ICU} + \Psi \tag{1}$$

where G_{IC} is the fracture energy, G_{ICU} is the fracture energy of the epoxy resin, and Ψ represents the overall toughening mechanisms. In the particular case of the fracture toughness experiments considered, the main toughening mechanisms are crack deflection, which resulted in a nonplanar crack, which induced a reduction in the driving force of the crack, and plastic void formation due to the matrix deformation around the thermoplastic particles. In such a case, the overall toughening contribution may be written as

$$\Psi = \Delta G_{cd} + \Delta G_v \tag{2}$$

where ΔG_{cd} is the contribution to the enhancement in fracture toughness from crack deflection, and ΔG_v is the contribution due to plastic void formation.

Faber and Evans[35] developed a model to predict the fracture improvement due to crack deflection around second-phase spherical particles. In this model, crack deflection resulted in crack fronts growing locally under modes I and II. The relative contribution to the energy release rate due to a portion of deflected crack front is obtained integrating over all the possible deviation angles from the original plane, θ. The energy release rate due to the entire crack front can be derived if the volume fraction of spheres, f, is known and is given by

$$G_{cd}^{sphere} = (1 + 0.87f)G_{ICU} \tag{3}$$

where G_{ICU} is the intrinsic toughness of the matrix. This model indicates that the fracture toughness enhancement due to crack deflection depends only on the volume fraction and particle shape but it is unchangeable with particle size. This expression can be written as a function of toughness increment:

$$\Delta K_{cd} = \sqrt{0.87f}K_{ICU} \tag{4}$$

where ΔK_{cd} is the increment in fracture toughness due to the crack deflection mechanism, and K_{ICU} is the fracture toughness of the pure epoxy resin.

The contribution to the increase in fracture energy from plastic void growth, ΔG_v, can be calculated using the following equation:[34]

$$\Delta G_v = \left(1 - \frac{\mu_m^2}{3}\right)(V_{fv} - V_{fr})K_{vm}^2\sigma_{yc}r_{yu} \tag{5}$$

where μ_m is a material constant and is normally taken to be 0.2 as reported in Ref. 12. V_{fv} is the volume fraction of voids and V_{fr} is equivalent to f, that is, the volume fraction of particles. K_{vm} is the maximum stress concentration factor of the von Misses stress in the epoxy resin and was found to be 2.22 around a void in an epoxy matrix.[12] σ_{yc} is the compressive yield stress of the epoxy resin and has been reported to be $\sim$ 100 MPa.[12] The radius of the plastic zone for the unmodified epoxy is r_{yu} and for its calculation has been assumed a circular plastic zone using the relationship:[1]

$$r_{yu} = \frac{1}{6\pi}\left(\frac{K_{Ic}}{\sigma_y}\right)^2 \tag{6}$$

where K_{Ic} is the fracture toughness of the epoxy resin and σ_y is the yield stress. The calculated value was of 5.55 μm.

The volume fraction of voids, V_{fv}, in the epoxy matrix was calculated principally from the detached particles and in a lesser extent, from the broken particles, which may have suffered debonding during the fracture. To get this magnitude, a deformation matrix index, k, was previously measured using the fracture surface micrographs as the following relationship:

$$k = 1 - \frac{A_p}{A_v} \tag{7}$$

where A_p is the area of the particle and A_v is the total area formed by the area of the void plus the area of the particle. From this expression, it can be inferred the volume fraction of voids, V_{fv}, which is related with the volume fraction of particles, V_{fr}:

$$V_{fv} = \frac{V_{fr}}{(1-k)^{3/2}} \tag{8}$$

Figure 10 compares the fracture toughness obtained from the different models with the experimental

results. It shows the experimental toughness, K_{IC}^{exp}, as a function of the PS-*co*-PA, together with the corresponding standard deviations, as well as the predicted fracture toughness assuming that the only mechanism involved is crack deflection, K_{cd}, and the calculated fracture toughness considering the plastic void growth as the only toughening mechanism, K_v. According to the fractography study, crack deflection accompanied by particles breakage is the main implicated mechanism in the fracture toughness enhancement, even though the predicted values due to this mechanism, K_{cd}, is slightly lower than the measured values. This points out that another mechanism must be acting. In a similar way, if plastic void growth around the overall PS-*co*-PA particles is estimated to be the only mechanism occurring, the predicted toughness, K_v, is a little higher than the experimental toughness.

Experimentally, it has been proved that the blends formed by a polystyrene copolymer present a good adhesion between the phases. This implies an increase in the fracture toughness with the PS-*co*-PA content because more energy is spent to divert the crack from its original plane followed by the breakage of the particles. The modeling of this mechanism predicted a fracture toughness slightly lower than the experimental values, which indicated that some other mechanism must be operating. The analysis of the fracture surfaces also revealed that the holes associated to the detached particles suffered plastic void growth and in a lesser extent, some of the broken particles. This behavior was the main toughening mechanism in the polystyrene/epoxy blends with poor adhesion between the phases investigated by Johnsen et al.[12] The average of detached or intact particles was of ~ 20% (Fig. 8), and so the necessary energy to fit the modeling fracture toughness due to the crack deflection mechanism with the experimental values is fulfilled with the contribution of these detached and broken particles.

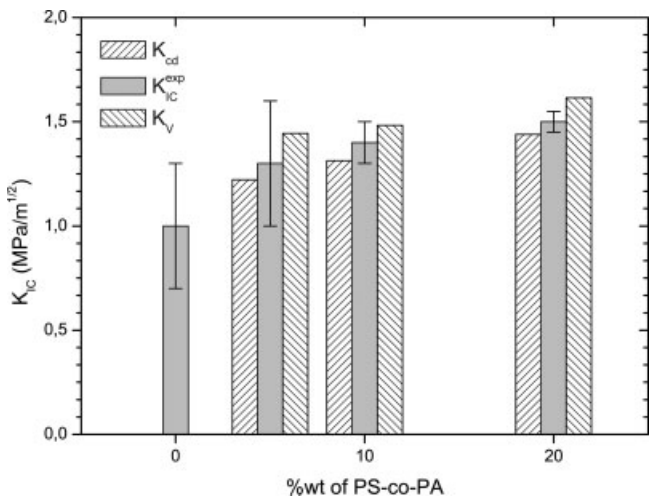

Figure 10 Measured values of fracture toughness, K_{IC}^{exp}, predicted fracture toughness due to crack deflection, K_{cd}, and calculated fracture toughness from void growth mechanism, K_v, as a function of the PS-*co*-PA content.

TABLE I
Volume Fraction (*f*) and Superficial Factor (*a*) of Particles of PS-*co*-PA

PS-*co*-PA (wt %)	*f*	*a*
5	0.056	0.044 ± 0.011
10	0.112	0.114 ± 0.015
20	0.222	0.140 ± 0.030

Annex

Table I gathers the volume fraction, *f*, and the superficial factor, *a*, of particles for each PS-*co*-PA content. The volume fraction was calculated using the following expression:

$$f_1 = \frac{\omega_1/\rho_1}{(\omega_1/\rho_1) + (\omega_2/\rho_2)} \quad (9)$$

where ω_i and ρ_i are the weight percentage and the density of the phase I, respectively. The densities of the DGEBA/DDS and the PS-*co*-PA are 1.237 and 1.083 g/cm^3,[20] respectively. On the other hand, the superficial factor of particles for each PS-*co*-PA content was obtained as the ratio between the total area of the PS-*co*-PA particles and the total area of the image. This magnitude includes the average values and the standard deviations corresponding to the measurements in three images. These data have not corrected by any factor to prevent the parallax error.

As the table shows, the superficial factor of particles and the volume fraction for the specimens with 5 and 10 wt % of PS-*co*-PA are in good agreement. The major differences are found in the blends with 20 wt % of PS-*co*-PA. Probably, these measurements are affected by parallax errors as the density of particles has increased.

CONCLUSIONS

The tensile properties and the fracture toughness at moderate high loading rates has been investigated in the blends formed by epoxy resin thermoset and poly(styre-*co*-allylalcohol) (PS-*co*-PA) copolymer as thermoplastic modifier. Apart from a two-phase morphology, the special feature of this system is the good adhesion between the dispersed thermoplastic particles and the epoxy resin matrix due to the copolymer presence in contrast to the epoxy/polystyrene blends.

The tensile strength and the deformation at break increased with the PS-*co*-PA content whereas the Young's modulus suffered no modification for this specific configuration. The fracture surfaces study revealed that this improvement was related to the increase of the roughness of the surface due to a crack deflection mechanism.

The fracture toughness at moderate loading rates increased with the PS-*co*-PA content. The maximum improvement was obtained in blends with a 20 wt % of PS-*co*-PA content and was 50% higher than that of the epoxy resin. Various mechanisms were responsible for the enhancement in fracture toughness, although the fracture surfaces revealed that the crack deflection was the dominant mechanism. The fractographic study also showed that $\sim$ 80% of the particles were broken, which corroborated the presence of a good adhesion between the phases. Besides, the holes related to detached particles presented plastic void growth and in a lesser extent, some of the broken particles. The modeling of the fracture toughness due to crack deflection predicted values slightly smaller than the experimental results. This implies that the plastic void deformation around detached particles must also contribute to the fracture energy although in a much less significant way as only 20% of the particles are detached.

References

1. Kinloch, A. J.; Young, R. J. Fracture Behaviour of Polymers; Elsevier Applied Science: London, 1983.
2. McGarry, F. J. Proc R Soc Lond A 1970, 319, 59.
3. Sultan, J. N.; McGarry, F. J. Polym Eng Sci 1973, 13, 29.
4. Meeks, A. C. Polymer 1974, 15, 675.
5. Yee, A. F.; Pearson, R. A. J Mater Sci 1986, 21, 2462.
6. Pearson, R. A.; Yee, A. F. J Mater Sci 1986, 21, 2475.
7. Pearson, R. A.; Yee, A. F. J Mater Sci 1989, 24, 2571.
8. Hedrick, J. C.; Patel, N. M.; McGrath, J. E. In Toughened Plastic. I. Science and Engineering; Riew, C. K., Kinloch, A. J., Eds.; American Chemical Society: Washington, 1993.
9. Malanga, M. Adv Mater 2000, 12, 1869.
10. Ritzenthalev, S.; Girard-Reydet, E.; Pascault, J. P. Polymer 2000, 41, 6375.
11. Korenberg, C. F.; Kinloch, A. J.; Taylor, A. C.; Schut, J. J Mater Sci Lett 2003, 22, 507.
12. Johnsen, B. B.; Kinloch, A. J.; Taylor, A. C. Polymer 2005, 46, 7352.
13. Bucknall, C. B.; Gilbert, A. H. Polymer 1989, 30, 213.
14. Frounchi, M. Eur Polym J 2001, 37, 995.
15. Hedrick, J. L.; Yilgor, I.; Jurek, M.; Hedrick, J. C.; Wilkes, G. L.; McGrath, J. E. Polymer 1991, 32, 2020.
16. Hourston, D. J.; Lane, J. M. Polymer 1992, 33, 1379.
17. Cardwell, B. J.; Yee, A. F. J Mater Sci 1998, 33, 5473.
18. Girard-Reydet, E.; Sautereau, H.; Pascault, J. P. Polymer 1999, 40, 1677.
19. Galante, M. J.; Borrago, J.; Williams, R. J. J.; Girard-Reydet, E.; Pascualt, J. P. Macromolecules 2001, 34, 2686.
20. Prolongo, S. G.; Salazar, A.; Rodríguez, J. Polym Eng Sci, in press.
21. Pavan, A. In Fracture Mechanics Testing Methods for Polymers, Adhesives and Composites, 1st ed.; Moore, D. R., Pavan, A., Williams, J. G., Eds.; Elsevier Science: The Netherlands, 2001.
22. Prolongo, S. G.; Burón, M.; Salazar, A.; Ureña, A.; Rodríguez, J. J Therm Anal Calorim 2007, 87, 269.
23. Oyanguren, P. A.; Frontini, P. M.; Williams, R. J. J.; Vigier, G.; Pascault, J. P. Polymer 1996, 37, 3087.
24. Giannotti, M. I.; Galante, M. J.; Oyanguren, P. A.; Vallo, C. I. Polym Test 2003, 22, 429.
25. Iijima, T.; Miura, S.; Fukuda, W.; Tomoi, M. Eur Polym J 1993, 29, 1103.
26. Grillet, A. C.; Galy, J.; Gérard, J. F.; Pascault, J. P. Polymer 1991, 32, 1885.
27. Abad, M. J.; Barral, L.; Cano, J.; López, J.; Nogueira, P.; Ramírez, C.; Torres, A. Eur Polym J 2001, 37, 1613.
28. Atsuta, M.; Turner, D. T. J Mater Sci Lett 1982, 1, 167.
29. Robertson, R. E.; Mindroiu, V. E. Polym Eng Sci 1987, 27, 55.
30. Fiedler, B.; Hojo, M.; Ochiai, S.; Schulte, K.; Ando, M. Compos Sci Technol 2001, 61, 1615.
31. Francis, B.; Thomas, S.; Jose, J.; Ramaswamy, R.; Lakshmana, Rao, V. Polymer 2005, 46, 12372.
32. Damani, R.; Gstrein, R.; Danzer, R. J Eur Ceram Soc 1996, 16, 695.
33. Picard, D.; Leguillon, D.; Putot, C. J Eur Ceram Soc 2006, 26, 1421.
34. Huang, Y.; Kinloch, A. J. J Mater Sci 1992, 27, 2763.
35. Faber, K. T.; Evans, A. G. Acta Metall 1983, 31, 565.